Received: 5 April 2021 | Revised: 20 July 2021 | Accepted: 21 July 2021

DOI: 10.1002/nbm.4599

RESEARCH ARTICLE

NMR IN BIOMEDICINE WILEY

Deuterium MRS of early treatment-induced changes in tumour lactate in vitro

Josephine L. Tan[1,2] | Daniel Djayakarsana[1,2] | Hanzhi Wang[1,2] | Rachel W. Chan[2] | Colleen Bailey[1,2,3] | Angus Z. Lau[1,2]

[1]Department of Medical Biophysics, University of Toronto, Toronto, Canada

[2]Physical Sciences Platform, Sunnybrook Research Institute, Toronto, Canada

[3]Department of Physics, Ryerson University, Toronto, Canada

Correspondence
Angus Z. Lau, Physical Sciences Platform, Sunnybrook Research Institute, 2075 Bayview Avenue, Room M7-600, Toronto, Ontario, Canada M4N 3M5.
Email: angus.lau@sri.utoronto.ca

Funding information
Natural Sciences and Engineering Research Council of Canada (NSERC), Grant/Award Numbers: RGPIN-2017-06596, RGPIN-2020-04765; Sunnybrook Foundation

Elevated production of lactate is a key characteristic of aberrant tumour cell metabolism and can be non-invasively measured as an early marker of tumour response using deuterium (^{2}H) MRS. Following treatment, changes in the ^{2}H-labelled lactate signal could identify tumour cell death or impaired metabolic function, which precede morphological changes conventionally used to assess tumour response. In this work, the association between apoptotic cell death, extracellular lactate concentration, and early treatment-induced changes in the ^{2}H-labelled lactate signal was established in an in vitro tumour model. Experiments were conducted at 7 T on acute myeloid leukaemia (AML) cells, which had been treated with 10 μg/mL of the chemotherapeutic agent cisplatin. At 24 and 48 h after cisplatin treatment the cells were supplied with 20 mM of [6,6′-$^2H_2$]glucose and scanned over 2 h using a two-dimensional ^{2}H MR spectroscopic imaging sequence. The resulting signals from ^{2}H-labelled glucose, lactate, and water were quantified using a spectral fitting algorithm implemented on the Oxford Spectroscopy Analysis MATLAB toolbox. After scanning, the cells were processed for histological stains (terminal deoxynucleotidyl transferase UTP nick end labelling and haematoxylin and eosin) to assess apoptotic area fraction and cell morphology respectively, while a colorimetric assay was used to measure extracellular lactate concentrations in the supernatant. Significantly lower levels of ^{2}H-labelled lactate were observed in the 48 h treated cells compared with the untreated and 24 h treated cells, and these changes were significantly correlated with an increase in apoptotic fraction and a decrease in extracellular lactate. By establishing the biological processes associated with treatment-induced changes in the ^{2}H-labelled lactate signal, these findings suggest that ^{2}H MRS of lactate may be valuable in evaluating early tumour response.

KEYWORDS
deuterium (^{2}H) MRS, treatment response, tumour lactate, Warburg effect

Abbreviations: ^{2}H, deuterium; ^{18}F-FDG, fluorine-18 fluorodeoxyglucose; AML, acute myeloid leukaemia; CT, computed tomography; H&E, haematoxylin and eosin; MCT, monocarboxylate transporter; OXSA, Oxford Spectroscopy Analysis; PBS, phosphate-buffered saline; PET, positron emission tomography; TUNEL, terminal deoxynucleotidyl transferase UTP nick end labelling..

This article was published online on 18 August 2021. Subsequently, the Funding Information was inadvertently removed and the correction was published on 27 August 2021.

1 | INTRODUCTION

Imaging plays a growing role in the non-invasive assessment of tumour response to treatment. For most solid tumours, the accepted clinical standard for response evaluation is based on the measurement of lesion size using computed tomography (CT) and MRI.[1,2] However, morphological changes may not occur until several weeks to months after treatment and do not always accurately reflect tumour progression or regression, rendering it difficult to assess early tumour response.[3,4] Imaging techniques that can detect early-stage markers of tumour response are therefore of great interest for optimizing subsequent therapy and reducing the burden of ineffective or unnecessary treatments.[5]

A potential early-stage imaging marker of treatment response is lactate.[6–8] In contrast to normal cells, tumour cells exhibit aberrant metabolism characterized by an increase in glycolysis regardless of aerobic conditions (known as the Warburg effect),[9] resulting in elevated lactate concentrations as high as 30 mM in multiple tumour types.[8] Following treatment, changes in lactate levels can provide insight into biological processes associated with response that precede gross changes in tumour size, including tumour cell death or impairment of metabolic function.[10]

Recently, deuterium (^{2}H) MRS was introduced as a potential clinical tool for imaging metabolism in vivo following the non-invasive administration of deuterated substrates such as glucose.[11–13] Compared with fluorine-18 fluorodeoxyglucose (^{18}F-FDG) positron emission tomography (PET), ^{2}H MRS can be performed on the same system as anatomical MRI scans, is non-radioactive, and informs on metabolism beyond glucose uptake. Given ^{2}H's low natural abundance (0.0115% of all naturally occurring hydrogen found on Earth), ^{2}H NMR spectra are minimally contaminated by background lipid and macromolecule signals. The predominant baseline water peak—before the administration of a ^{2}H-labelled substrate—can be used as an internal concentration reference. Moreover, the short T_1 relaxation times of ^{2}H provide increased SNR through signal averaging. The short T_2 relaxation time results in intrinsically broader NMR signals relative to ^{1}H, but this does not greatly impact the resulting spectral quality, as the ^{2}H NMR spectra derived from deuterated substrates contain only a few metabolite peaks.[11–13] By detecting downstream ^{2}H-labelled metabolites such as lactate, ^{2}H MRS has been shown to differentiate between normal and glioblastoma tissue in humans[12] and detect treatment response 48 h after chemotherapy in murine tumour models.[13] These findings demonstrate that changes in ^{2}H-labelled lactate may be valuable as an indicator of early tumour response, but the biological processes associated with this marker have not yet been established.

In this work, in vitro experiments were performed using ^{2}H MRS to assess any correlations between ^{2}H-MRS measures of lactate signal, extracellular lactate concentrations, and apoptotic cell death following chemotherapy. We show for the first time that significant decreases in the ^{2}H-lactate signal observed 48 h after treatment were associated with histologically confirmed apoptotic cell death and decreased extracellular lactate.

2 | METHODS

2.1 | Cell preparation

The experimental workflow is summarized in Figure 1. The acute myeloid leukaemia 5 (AML-5) cell line was chosen for this in vitro study because of the well documented apoptotic nature of its response to cisplatin.[14–18] AML cells were grown in suspension in 12 flasks containing 150 mL alpha minimum essential medium (Invitrogen Canada, Burlington, Canada), with 5% foetal bovine serum (Fisher Scientific, Ottawa, Canada), and 1% penicillin and streptomycin (Invitrogen Canada). Flasks were maintained at 37 °C and 5% CO_2 until they reached confluence (~10^6 cells/mL). To induce apoptosis, cells in each of the flasks were treated with 10 μg/mL cisplatin 24 or 48 h prior to imaging. A single sample was prepared by combining four flask volumes (~6 × 10^8 cells total), which were centrifuged at 3000 rpm for 15 min at 4 °C using a fixed angle centrifuge (Beckman Coulter, Brea, CA). After removal of excess supernatant, the pellet was resuspended in phosphate-buffered saline (PBS) and centrifuged at 2400 *g* for 10 min at 4 °C using a swinging bucket centrifuge (Thermo Electron, Asheville, NC). PBS was used to resuspend the pellet into an MR-compatible glass tube with a final volume of 600 μL. Each experiment utilized three samples. 10 min prior to the ^{2}H scan, 100 μL of 140mM [6,6′-$^2H_2$]glucose solution (Cambridge Isotope Laboratories, Tewksbury, MA) was added to each tube for a final ^{2}H-labelled glucose concentration

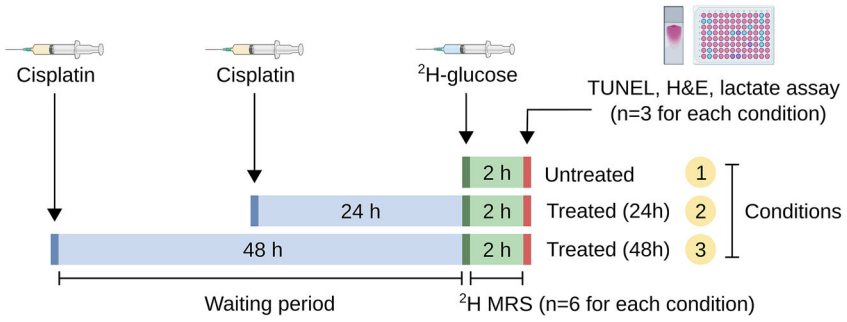

FIGURE 1 Schematic experimental timeline for the untreated and cisplatin-treated cells

of 20 mM (and final volume 700 μL) and mixed into the cell suspension with a micropipette. The experiment was repeated twice to determine reproducibility, and was performed with untreated samples and samples treated with cisplatin 24 and 48 h prior to scanning.

2.2 | ^{2}H MRS data acquisition

MR experiments were performed at 7 T (Bruker BioSpec 70/30 USR, Billerica, MA, USA). A home-built transmit/receive surface coil (46.1 MHz, diameter 20 mm) was used to acquire the ^{2}H signal. The coil included a proton blocking trap circuit to prevent the induction of currents on the ^{2}H coil by the ^{1}H body coil in the scanner. Three MR-compatible glass tubes (6 mm diameter × 50 mm length) containing the cell samples were placed side by side adjacent to the centre of the surface coil, as illustrated in Figure 2A. Magnetic field homogeneity was optimized by acquiring a B_0 field map and applying a second order shim using a shim box of volume 2 × 2 × 2 cm^3 placed manually to cover the extent of the tubes. ^{2}H excitation was achieved with a 90° rectangular RF pulse followed by 2D phase-encoding gradients. The flip angle was calibrated using separate phantom scans prior to in vitro scans. 2D ^{2}H MRS images were acquired at an in-plane resolution of 10 × 3 mm^2 and temporal resolution of 2 min (FOV = 8 × 3 cm^2, spectral width 3 kHz, 768 spectral points, flip angle = 90°, T_R = 300 ms, T_E = 0.551 ms, 300 averages). The rectangular voxels were chosen to match the length of the cell sample tubes. A single ^{2}H MRS image was first acquired to measure baseline metabolism before the cell samples were removed from the scanner and injected with deuterated glucose. Following the addition of glucose, the cell sample tubes were placed back onto the coil and reshimmed. 10 min after the injection of glucose, dynamic ^{2}H MRS images were acquired over 120 min. Proton T_1-weighted GRE images at an in-plane resolution of 0.03125 × 0.03125 cm^2 (FOV = 8 × 8 cm^2, T_R = 60 ms, T_E = 2 ms) were acquired with the ^{1}H volume coil.

2.3 | ^{2}H MR data analysis

The spectrum for each sample tube was chosen from the voxel in the most sensitive region of the surface coil with the highest SNR. Apodization of the raw data was achieved with a 5 Hz window function in the time domain and performing a Fourier transform. The spectra were then zero-order phase-corrected. Spectra were averaged from every 12 min of data acquisition (corresponding to 30 images) to maximize SNR. Spectral fitting was performed using the Advanced Method for Accurate, Robust and Efficient Spectral Fitting (AMARES) algorithm implemented in the Oxford Spectroscopy Analysis (OXSA) MATLAB toolbox.[19] The fitting model is constrained by prior knowledge including the relative chemical shifts (bounded by ±0.2 ppm) and linewidths. A single Lorentzian line shape was fitted to each metabolite, as there was no evidence of multiple

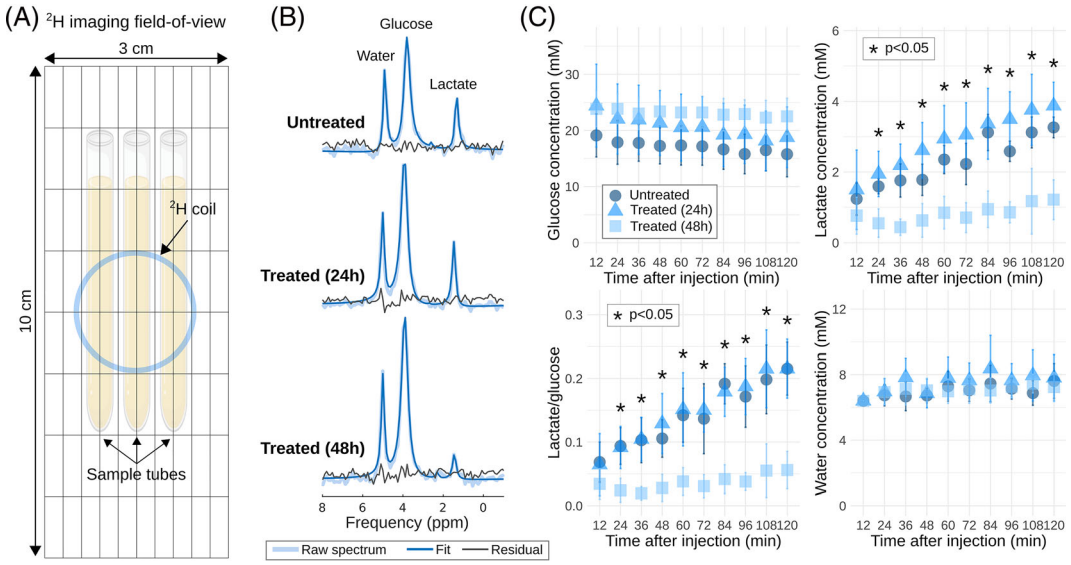

FIGURE 2 A, Experimental setup consisting of three AML sample tubes lying on top of the ^{2}H surface coil (blue circle), with overlaid 2D matrix. B, Representative single voxel ^{2}H spectra for the untreated and cisplatin-treated samples 2 h after injection of [6,6′-^{2}H$_2$]glucose. Spectra are averaged over 12 min of acquisition. C, Time course of ^{2}H-labelled glucose, lactate, lactate/glucose, and water concentrations 10 min after injection of [6,6′-^{2}H$_2$]glucose. Error bars are the standard deviations across six samples. Asterisks indicate statistically significant differences between the 48 h treated and untreated samples, and between the 48 h and 24 h treated samples (p < 0.05)

peaks with the linewidths observed. Metabolite signals were quantified by area integration of the peaks,[19] which included ^{2}H-labelled glucose (3.7 ppm), glutamate and glutamine (Glx, 2.4 ppm), lactate (1.4 ppm), and water (4.7 ppm). The fitting was bound between ±0.1 ppm. These chemical shifts were taken from literature[11–13] and verified from our spectral fitting. For display, ^{2}H MRS maps were resampled and overlaid onto the corresponding proton T_1-weighted image.

Signals were corrected by a factor that accounted for partial signal saturation, given by

$$S_0 = \frac{S}{\left(1-\exp\left(-\frac{T_R}{T_1}\right)\right)\sin\theta / \left(1-\cos\theta\exp\left(-\frac{T_R}{T_1}\right)\right)}$$

where S and S_0 are the signal before and after correction, respectively, T_R is the repetition time [ms], T_1 is the longitudinal relaxation [ms], θ is the prescribed flip angle [rad], and T_E is the echo time [ms]. The T_1 values of ^{2}H-labelled metabolites were based on in vivo values from literature measured at 7 T (Reference 12): 64 ms (glucose), 146 ms (Glx), 297 ms (lactate), and 320 ms (water). Concentrations of labelled glucose and lactate were quantified by normalizing the integrals of the fitted peaks to that of the baseline water signal, which has a natural ^{2}H abundance of 12.8 mM. This value is based on the 55.5 M concentration of water, the two protons of the water molecule, and 0.0115% natural abundance of ^{2}H. As described by de Feyter et al,[12] the absolute concentrations of glucose, Glx, lactate, and water were determined by normalizing to the average number of deuterons per molecule (glucose 2, Glx 1.33, lactate 3, water 2). Tukey's post hoc test was used to determine statistically significant differences ($p < 0.05$) in metabolite concentrations between the untreated and cisplatin-treated samples at each time point (12, 24, 36, 48, 60, 72, 84, 96, 108, 120 min) following glucose injection. Statistical calculations were performed with R (v4.0.3: R Core Team [2020], Vienna, Austria).

2.4 | In vitro assays

^{2}H MRS data were compared with cell sample histology and lactate assay measurements. Immediately following ^{2}H MRS, three samples from each treatment category (untreated, 24 h treated, and 48 h treated) were transferred into 1.5 mL Eppendorf tubes and centrifuged at 2400 g for 10 min. 300 μL of supernatant was extracted from each tube and stored at −80 °C for at least 48 h for lactate assays. To prepare samples for histology, pellets were fixed in 10% formalin for at least 96 h. The pellets were embedded in 3% agarose gel and stained with terminal deoxynucleotidyl transferase UTP nick end labelling (TUNEL) and H&E to assess apoptotic area and cell morphology, respectively (University Health Network Pathology Research Program, Toronto, Canada). Slides were examined under a light microscope (×10 and ×200 magnification). ImageJ2[20] was used to measure the percent area of TUNEL positive (TUNEL$^+$) staining in three fields of view of each slide.

The supernatant lactate concentration was measured using a lactate colorimetric assay kit (K607, BioVision, Milpitas, CA) according to the manufacturer's instructions. For sample preparation, 0.8 μL of the supernatant was added per well. Tukey's post hoc test was used to determine statistically significant differences ($p < 0.05$) between the untreated and cisplatin-treated samples for ^{2}H-labelled lactate concentrations at the last MRI time point (120 min), and corresponding TUNEL$^+$ staining and supernatant lactate concentrations.

3 | RESULTS

The ^{2}H spectra acquired 2 h after the injection of [6,6′-^{2}H$_2$]glucose in the untreated and cisplatin-treated samples are presented in Figure 2B. The spectra were averaged from a 12 min window. Shimming resulted in a linewidth of 15 to 20 Hz (0.050 to 0.070 ppm). The spectra were well described by the fitted spectral model, as indicated by the output Cramér-Rao lower bounds, which measure the uncertainty in the fit.[19] Signals were observed from deuterated water (4.7 ppm), the injected glucose (3.7 ppm), and downstream lactate (1.4 ppm). No Glx was detected in either the cisplatin-treated or untreated groups. Figure 2C shows the concentration of deuterated water and the ^{2}H-labelled metabolites over 2 h, 10 min after ^{2}H-glucose administration, averaged across six samples. The 48 h treated sample exhibited reduced glucose metabolism, as indicated by steady concentrations of glucose and lactate over time. In contrast, glucose levels decreased while lactate levels increased over the 2 h time course of the 24 h treated and untreated samples. Across six samples, a significantly lower lactate concentration was detected at all time points beyond 12 min (up to 120 min) after glucose administration in the 48 h treated cells compared with the untreated ($p < 0.05$) and with the 24 h treated cells ($p < 0.05$). Similar trends were observed in the time course of lactate/glucose ratios, where the ratios were significantly lower in the 48 h treated cells compared with the untreated ($p < 0.05$) and with the 24 h treated cells ($p < 0.05$) at all time points beyond 12 min after glucose injection. No significant differences in lactate or lactate/glucose were detected between the untreated and 24 h treated samples at any time point ($p > 0.05$). There were also no significant differences detected in glucose or water concentration at any time point between any of the samples. Figure 3 shows representative 2D spectroscopic images of metabolite signals 2 h after glucose administration. Reduced lactate signal was observed in the 48 h treated samples compared with the untreated and 24 h treated samples.

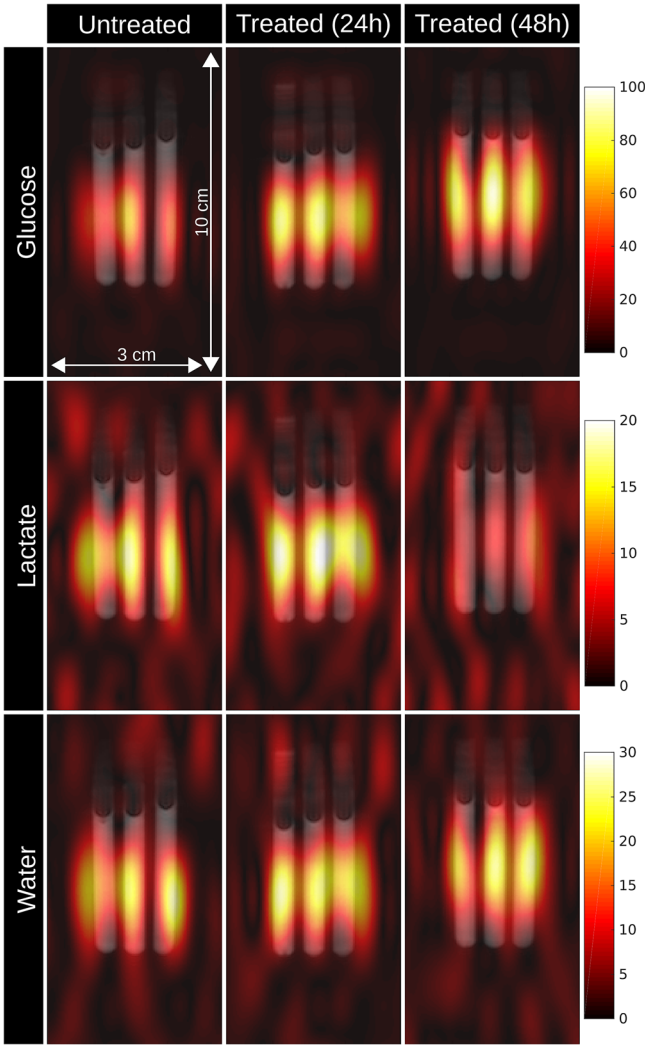

FIGURE 3 Representative ^{2}H spectroscopic images overlaid on T_1 images 2 h after injection of [6,6′-$^{2}H_2$]glucose. The spectral data were averaged over 12 min of acquisition. The untreated, 24 h treated, and 48 h treated spectroscopic images shown were acquired from three separate experiments. Colour bars represent arbitrary signal intensity

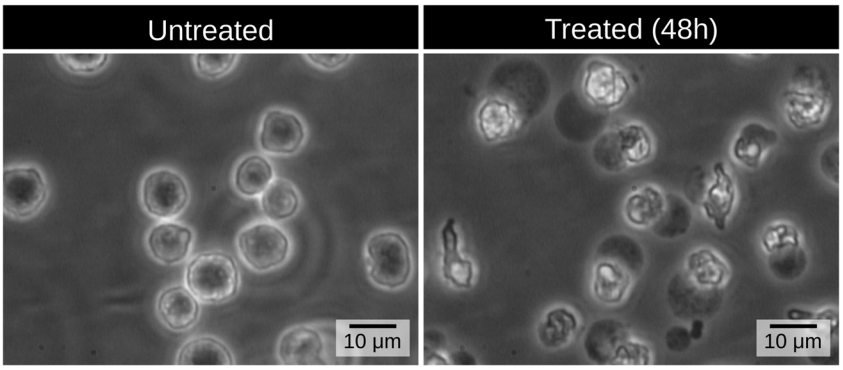

FIGURE 4 Phase contrast microscope images of AML cells in suspension. Cells are approximately 10 μm in diameter. Apoptotic changes can be observed 48 h after treatment, including nuclear condensation, membrane blebbing, and cell size shrinkage

Figure 4 shows a microscope image of AML cells in suspension, which are approximately 10 μm in diameter. Apoptotic changes are evident 48 h after treatment with cisplatin, such as nuclear condensation, membrane blebbing, and cell size shrinkage. These characteristics are reflected in the histology slides shown in Figure 5. Cell size shrinkage may have been caused by formalin fixation. The haematoxylin and eosin (H&E)

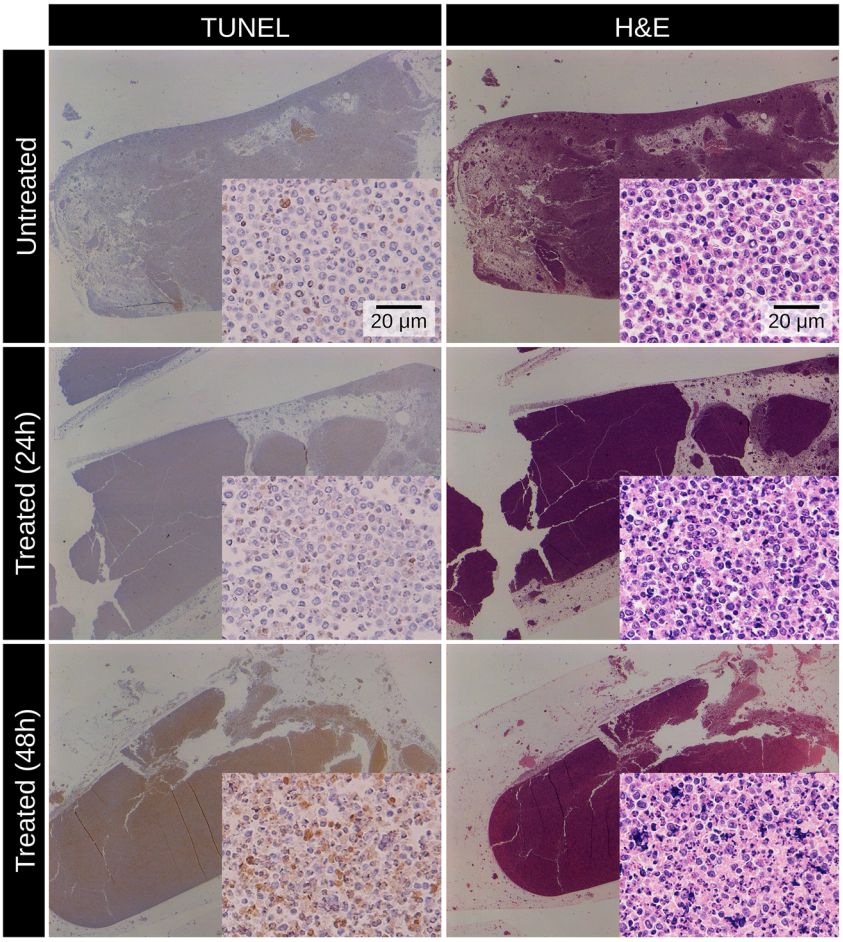

FIGURE 5 Representative TUNEL and H&E stained sections (×10 and ×200 magnification) from untreated and cisplatin-treated cell pellets, which were fixed in formalin for at least 96 h after scanning. Formalin fixation may have caused cell shrinkage

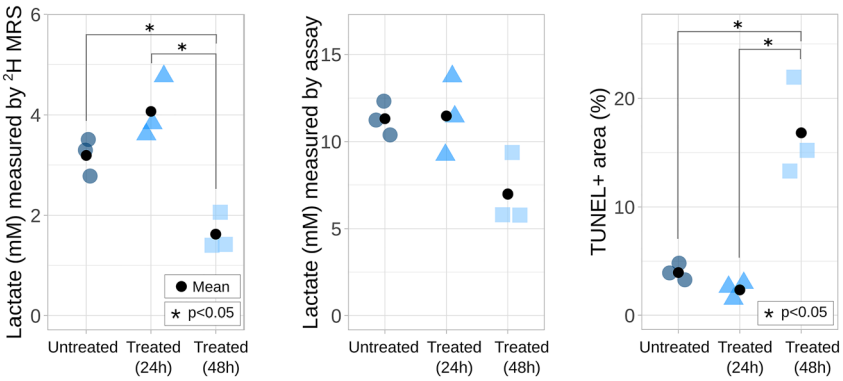

FIGURE 6 Comparison of ^{2}H-lactate measured using ^{2}H MRS 120 min after glucose injection, and corresponding assay measurements of lactate in supernatant and TUNEL positive percent area across three samples. ^{2}H-lactate data are averaged from 12 min of data acquisition. Statistically significant differences ($p < 0.05$) were determined using Tukey's post hoc test

sections of the 48 h treated cells showed increased nuclear fragmentation, evidenced by dark purple clusters, compared with the untreated and 24 h treated cells. Similarly, the TUNEL sections of the 48 h treated cells showed increased positive staining, which appear as brown regions, compared with the untreated and 24 h treated cells. Figure 6 compares the lactate concentrations measured using ^{2}H MRS 2 h after glucose injection from three samples, and corresponding lactate measurements from the assay and TUNEL^{+} area fraction from the histology slides. Across the three samples 2 h after glucose injection, ^{2}H-labelled lactate concentration was significantly lower in the 48 h treated sample (1.6 ± 0.4 mM)

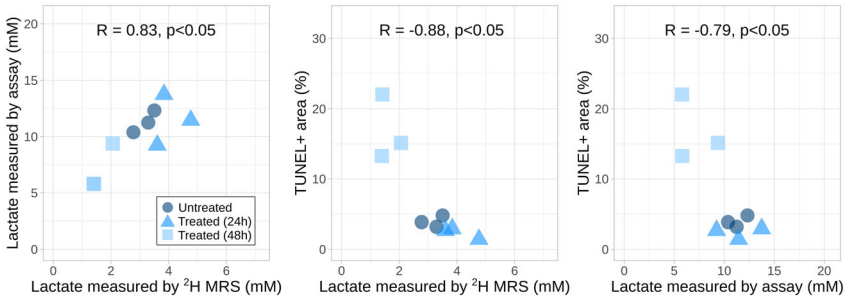

FIGURE 7 Significant correlations were determined between the lactate MRS and assay measurements, the MRS measurements and TUNEL positive percent area (TUNEL$^+$ area), and the assay measurements and TUNEL$^+$ area ($p < 0.05$). *R* represents Pearson's correlation coefficient

compared with the untreated (3.2 ± 0.4 mM, $p < 0.05$) and 24 h treated samples (4.0 ± 0.6 mM, $p < 0.05$). There was no significant difference detected in ^{2}H MRS lactate measurements between the untreated and 24 h treated samples ($p > 0.05$). The lactate assay of the sample supernatants indicated that there was less extracellular lactate in the 48 h treated sample (7.0 ± 2.1 mM) compared with untreated (11.3 ± 1.0 mM) and 24 h treated samples (11.5 ± 2.3 mM). However, the differences were not significant between any group ($p > 0.05$). In contrast, there was a significantly greater TUNEL$^+$ area in the 48 h treated cell pellet histology slides (16.8 ± 4.6%) compared with the untreated (3.9 ± 0.8%, $p < 0.05$) and 24 h treated slides (2.3 ± 0.8%, $p < 0.05$). Like the ^{2}H MRS lactate measurements, there was no significant difference in TUNEL$^+$ area between the untreated and 24 h treated samples ($p > 0.05$). Figure 7 shows the correlation plots between ^{2}H MRS lactate measurements, lactate assay measurements, and TUNEL$^+$ area fraction. The ^{2}H MRS lactate levels were significantly correlated with the assay measurements ($p < 0.05$). Both MRS and assay lactate data were significantly negatively correlated with the TUNEL$^+$ area fraction ($p < 0.05$).

4 | DISCUSSION

In this study, the metabolic changes in cisplatin-treated AML cells were measured using ^{2}H MRS and correlated with biological parameters including extracellular lactate concentration and apoptotic area fraction. Consistent with the Warburg effect[9] and previous ^{2}H MRS studies of glucose metabolism in tumours,[12,13] the AML cells demonstrated metabolic conversion of glucose into lactate. This change was observed within 2 h following the administration of ^{2}H-labelled glucose, in agreement with other dynamic ^{2}H MRS studies.[11,13] Little to no Glx signal was observed, indicating low TCA cycle flux. Beyond 12 min after glucose administration, there was a significant decrease in ^{2}H-labelled lactate production in the samples treated with cisplatin 48 h prior to scanning, relative to the untreated samples and 24 h treated samples. No significant differences in glucose concentrations were observed at any time point between any of the samples, although glucose utilization appeared reduced in 48 h treated cells compared with the untreated and 24 h treated cells. Similarly, there were no significant differences in water concentrations. This observation may be explained by the low TCA cycle flux and the in vitro nature of the experiment, since the accumulation of ^{2}H-labelled water has been shown to arise from label transfer to water during several reactions in the TCA cycle[12,13] and wash-in of labelled water from other tissues in vivo.[13]

To account for the potential variation in ^{2}H-glucose dosage and/or viable cell population within the sample, labelled lactate/glucose over time was also examined. The lactate/glucose ratio was significantly lower in the 48 our treated samples compared with both the untreated and 24 h treated samples beyond 12 min after injection of labelled glucose. At 120 min after injection of labelled glucose, the lactate/glucose ratios across six samples for the untreated cells (0.22 ± 0.04) and 48 h treated cells (0.06 ± 0.03) were lower than ^{2}H-labelled lactate/glucose ratios measured in EL4 tumour bearing mice 48 h after treatment with etoposide (0.27 ± 0.12 to 0.12 ± 0.06).[13] Reasons for this discrepancy might include the difference between cell lines, chemotherapeutic agents and doses, and variations arising from in vivo versus in vitro measurements such as oxygen supply and availability of glucose.

Lactate concentrations quantified by ^{2}H MRS were compared with measurements of extracellular lactate concentration from a colorimetric assay. In agreement with the ^{2}H MRS data, extracellular lactate concentrations were lower in the 48 h treated sample compared with the untreated and 24 h treated samples. Extracellular assay-based lactate concentrations were significantly correlated to those measured by ^{2}H MRS two hours after glucose administration ($R = 0.83$, $p < 0.05$). In addition, we found that the extracellular lactate concentrations were an average of 3.6 times higher than the ^{2}H MRS measurements, which reflect the total ^{2}H labelled lactate in the cell suspension 2 h after glucose administration, referenced to the 12.8 mM baseline concentration of natural abundance ^{2}H-water. This finding is consistent with high levels of monocarboxylate transporter 4 (MCT4)-mediated lactate export leading to higher extracellular versus intracellular lactate concentrations.[6,8] Several other factors may also contribute to this discrepancy. First, the cell fraction by volume was measured to be approximately 40% (corresponding to an approximate 400 μL supernatant volume in 700 μL total sample volume). The cells may have also continued to metabolize glucose into lactate during the 30 min delay time following the MR scan needed to prepare the sample supernatant for the assay. Finally, unlabelled lactate in the supernatant produced from unlabelled glucose in residual cell medium would be detected by the assay but not by ^{2}H MRS. From Figure 7, the extrapolated

y intercept is 4.1 mM ($p < 0.05$) and presumably represents the unlabelled lactate in the sample. In future experiments, the colorimetric assays should be performed on lysed cells to include the lactate contribution from both intracellular and extracellular spaces.

The decrease in lactate concentration, as measured by both ^{2}H MRS and the lactate assay, was significantly correlated with the histologically confirmed increase in percent area of TUNEL positive staining 48 h after cisplatin was administered. The 48 h treated samples also demonstrated morphological features of apoptosis in H&E-stained sections such as DNA fragmentation. These findings suggest that an increase in cisplatin-induced apoptosis results in a decrease in lactate production since there are fewer viable cells to metabolize the administered glucose. Interestingly, the metabolic and apoptotic effects of cisplatin were not detected in the 24 h treated cells by either ^{2}H MRS, the colorimetric assay, or TUNEL. However, an early stage of apoptosis, characterized by nuclear condensation, is apparent in the H&E stains of the 24 h treated samples. This observation suggests that the apoptotic effects of cisplatin have been initiated by this time point but have not yet manifested in metabolic changes or DNA fragmentation. Since cisplatin affects the ability of the cell to divide by creating DNA crosslinks,[21] these effects may only become more apparent after the doubling time of the AML cells (~31 h).[15]

Given the percent of viable cells in the untreated (~95%) and 48 h treated (~85%) samples (approximated from the TUNEL positive percent area), the change in lactate concentration between these two groups is greater than expected (~0.3 mM expected versus 1.6 mM measured by ^{2}H MRS and 4.3 mM measured by assay). The observed drop in lactate concentration may be attributed to other cisplatin-mediated mechanisms in addition to apoptosis, such as a "stun" in glucose metabolism from disrupted cell machinery. Cisplatin, a chemotherapeutic drug known to exert cytotoxicity by apoptosis, has also been postulated to act as an anti-metabolic agent. Cisplatin has been found to suppress the expression of glycolysis-related proteins including glucose transporters 1 and 4 (GLUT1 and GLUT4) and lactate dehydrogenase B (LDHB), leading to a decline in glucose uptake and lactate production in vitro.[22] There may also be reduced expressions of other proteins involved in glycolysis such as MCTs and lactate dehydrogenase A (LDHA), which facilitate the transport of lactate into and out of the cell and the bidirectional conversion of pyruvate to lactate, respectively.[8,23] These factors may affect lactate production before TUNEL staining can indicate apoptotic cell death. Western blot analysis of these protein levels in future ^{2}H MRS studies may add valuable information regarding the mechanisms of the observed metabolic change.

The setup of this experiment consisted of a plane of three tubes placed horizontally above the centre of a ^{2}H surface coil. This layout enabled sufficient signal acquisition using a 2D CSI sequence. Sensitivity was the greatest in the centre of the coil, leading to a high signal in a single voxel from each tube. For this reason—and to prevent potential signal contamination from neighbouring voxels—only these three voxels were chosen for analysis. In our case, 2D maps obtained via spectroscopic imaging served to demonstrate the spatial resolution and localization of the ^{2}H signal relative to the coil within the three identical sample tubes. In a clinical application, these metabolic maps have been shown to distinguish between normal and aberrant metabolism with striking contrast.[12] Using 3D ^{2}H MRS maps of glucose, lactate, and Glx, de Feyter et al have demonstrated elevated lactate and reduced Glx in a glioma relative to normal brain tissue.[12] Given the nominal voxel size of $2 \times 2 \times 2$ mm^{3} used in this study, these ^{2}H MRS metabolic maps could be used to provide a quantitative assessment of response across the tumour volume and capture the presence of spatial metabolic heterogeneities that may further inform on tumour status. Due to its ability to map metabolites downstream of glucose, ^{2}H MRS overcomes a major disadvantage of ^{18}F-FDG PET which is limited to imaging glucose uptake.[10]

Some technical limitations of ^{2}H MRS should be considered. As for carbon-13 (^{13}C) MR, an existing clinical MRI scanner would require specialized multinuclear hardware.[12] However, additional complexities such as hyperpolarization or water and lipid suppression are not necessary for ^{2}H MRS. In addition, the ^{2}H-labelled substrates are cheaper than those used in ^{13}C MR and can be orally ingested rather than injected.[12] The long scan time and high field strength used in our study have major cost and impracticality, but our results demonstrate that significant metabolic differences between samples can be detected after 12 min after glucose addition. Furthermore, an adequate shim of 0.05-0.07 ppm was achieved in these in vitro experiments, which is not feasible in vivo. However, multiple studies have demonstrated that ^{2}H MRS can be implemented to study metabolism in vivo.[11–13] For example, de Feyter et al achieved an 11 Hz water linewidth in the human brain and were able to differentiate normal and tumour metabolism within a 30 min scan at a lower field strength of 4 T.[12]

As this study was performed in vitro, some factors should be considered when interpreting the observed metabolic changes. First, the experiment was performed at room temperature instead of at the physiologically relevant temperature of 37 °C. The concentration of glucose administered is also four times that found in normal blood. While temperature[24] and glucose availability[25] have been shown to impact the metabolic rates of tumour cells in vitro, these conditions were consistent between our samples such that there was still a clear effect of cisplatin on the metabolism of the 48 h treated cells compared with the untreated group. Kinetic analysis of dynamic ^{2}H MRS should be included in future work to compare glucose consumption and lactate production rates with those found in physiological conditions. Second, the varying number of cell passages may introduce genetic drift and cause differences in morphology, growth rates, and protein expression.[26] However, the MR and biological data show consistent metabolic trends across the untreated, 24 h treated, and 48 h treated groups, suggesting that the effect of passaging on metabolism and cell death was likely minor. Future experiments should include vehicle-treated samples to control for passage number and reduce experimental variance in the untreated and treated groups. Finally, our technique was tested on a single AML cell line, which, being cancer of the blood, is not assessed for response via anatomical changes as done in solid tumours.[27] However, these cells were chosen for proof of concept as they are highly glycolytic[28] and have an apoptotic response to cisplatin.[14–18] Accordingly, the AML cells depicted the Warburg effect similarly to the metabolic profiles found in a murine lymphoma model,[13] a glioma

model,[12] and patients with glioblastoma multiforme[12] using ^{2}H MRS. Our in vitro approach permitted us to study this effect and the resulting changes in lactate induced by cisplatin without confounding effects from tumour vasculature or the extracellular matrix, which introduce additional complexity for metabolite quantification.[11,13]

5 | CONCLUSIONS

Increased lactate levels are a consequence of aberrant metabolism exhibited by many tumour types that contribute to the survival and metastatic potential of tumour cells. The results of this work showed that significant treatment-induced changes in lactate can be detected by ^{2}H MRS as early as 48 h after chemotherapy and were associated with changes in extracellular lactate levels and apoptotic cell death. These findings suggest that ^{2}H-labelled lactate may be used in the assessment of tumour response early after treatment. Protein analysis in future work is warranted to determine the mechanisms of the observed metabolic change.

ACKNOWLEDGEMENTS

The authors gratefully acknowledge funding from NSERC (RGPIN-2017-06596, RGPIN-2020-04765). The AML-5 cell line was kindly provided by Dr Gregory Czarnota (Sunnybrook Health Sciences Centre).

DATA AVAILABILITY STATEMENT

The data that support the findings of this study are available from the corresponding author upon reasonable request.

ORCID

Josephine L. Tan https://orcid.org/0000-0003-2437-1044
Angus Z. Lau https://orcid.org/0000-0002-9604-394X

REFERENCES

1. Therasse P, Arbuck SG, Eisenhauer EA, et al. New guidelines to evaluate the response to treatment in solid tumors. *J Natl Cancer Inst*. 2000;92(3):205-216. https://doi.org/10.1093/jnci/92.3.205
2. Eisenhauer EA, Therasse P, Bogaerts J, et al. New response evaluation criteria in solid tumours: revised RECIST guideline (version 1.1). *Eur J Cancer*. 2009;45(2):228-247. https://doi.org/10.1016/j.ejca.2008.10.026
3. Brindle K. New approaches for imaging tumour responses to treatment. *Nat Rev Cancer*. 2008;8(2):94-107. https://doi.org/10.1038/nrc2289
4. Michaelis LC, Ratain MJ. Measuring response in a post-RECIST world: from black and white to shades of grey. *Nat Rev Cancer*. 2006;6(5):409-414. https://doi.org/10.1038/nrc1883
5. Campbell A, Davis LM, Wilkinson SK, Hesketh RL. Emerging functional imaging biomarkers of tumour responses to radiotherapy. *Cancer*. 2019;11(2):131. https://doi.org/10.3390/cancers11020131
6. Hirschhaeuser F, Sattler UGA, Mueller-Klieser W. Lactate: a metabolic key player in cancer. *Cancer Res*. 2011;71(22):6921-6925. https://doi.org/10.1158/0008-5472.CAN-11-1457
7. San-Millán I, Brooks GA. Reexamining cancer metabolism: lactate production for carcinogenesis could be the purpose and explanation of the Warburg Effect. *Carcinogenesis*. 2017;38(2):119-133. https://doi.org/10.1093/carcin/bgw127
8. de la Cruz-López KG, Castro-Muñoz LJ, Reyes-Hernández DO, García-Carrancá A, Manzo-Merino J. Lactate in the regulation of tumor microenvironment and therapeutic approaches. *Front Oncol*. 2019;9:1143. https://doi.org/10.3389/fonc.2019.01143
9. Warburg BYO, Wind F. The metabolism of tumors in the body. *J Gen Physiol*. 1926;8(6):519-530.
10. Pantel AR, Ackerman D, Lee SC, Mankoff DA, Gade TP. Imaging cancer metabolism: underlying biology and emerging strategies. *J Nucl Med*. 2018;59(9):1340-1349. https://doi.org/10.2967/jnumed.117.199869
11. Lu M, Zhu XH, Zhang Y, Mateescu G, Chen W. Quantitative assessment of brain glucose metabolic rates using in vivo deuterium magnetic resonance spectroscopy. *J Cereb Blood Flow Metab*. 2017;37(11):3518-3530. https://doi.org/10.1177/0271678X17706444
12. de Feyter HM, Behar KL, Corbin ZA, et al. Deuterium metabolic imaging (DMI) for MRI-based 3D mapping of metabolism in vivo. *Sci Adv*. 2018;4(8):eaat7314-eaat7336. https://doi.org/10.1126/sciadv.aat7314
13. Kreis F, Wright A, Hesse F, Fala M, Hu D, Brindle K. Measuring tumor glycolytic flux in vivo by using fast deuterium MRI. *Radiology*. 2019;294(2):289-296. https://doi.org/10.1148/radiol.2019191242
14. Bailey C, Giles A, Czarnota GJ, Stanisz GJ. Detection of apoptotic cell death in vitro in the presence of Gd-DTPA-BMA. *Magn Reson Med*. 2009;62(1):46-55. https://doi.org/10.1002/mrm.21972
15. Bailey C, Desmond KL, Czarnota GJ, Stanisz GJ. Quantitative magnetization transfer studies of apoptotic cell death. *Magn Reson Med*. 2011;66(1):264-269. https://doi.org/10.1002/mrm.22820
16. Portnoy S, Fichtner ND, Dziegielewski C, Stanisz MP, Stanisz GJ. In vitro detection of apoptosis using oscillating and pulsed gradient diffusion magnetic resonance imaging. *NMR Biomed*. 2014;27(4):371-380. https://doi.org/10.1002/nbm.3070
17. Vlad RM, Alajez NM, Giles A, Kolios MC, Czarnota GJ. Quantitative ultrasound characterization of cancer radiotherapy effects in vitro. *Int J Radiat Oncol Biol Phys*. 2008;72(4):1236-1243. https://doi.org/10.1016/j.ijrobp.2008.07.027
18. Farhat G, Yang VXD, Czarnota GJ, Kolios MC. Detecting cell death with optical coherence tomography and envelope statistics. *J Biomed Opt*. 2011;16(2):026017. https://doi.org/10.1117/1.3544543

19. Purvis LAB, Clarke WT, Biasiolli L, Valkovič L, Robson MD, Rodgers CT. OXSA: an open-source magnetic resonance spectroscopy analysis toolbox in MATLAB. *PLoS ONE*. 2017;12(9):e0185356. https://doi.org/10.1371/journal.pone.0185356
20. Rueden CT, Schindelin J, Hiner MC, et al. ImageJ2: ImageJ for the next generation of scientific image data. *BMC Bioinformatics*. 2017;18:529. https://doi.org/10.1186/s12859-017-1934-z
21. Dasari S, Bernard Tchounwou P. Cisplatin in cancer therapy: molecular mechanisms of action. *Eur J Pharmacol*. 2014;740:364-378. https://doi.org/10.1016/j.ejphar.2014.07.025
22. Wang S, Xie J, Li J, Liu F, Wu X, Wang Z. Cisplatin suppresses the growth and proliferation of breast and cervical cancer cell lines by inhibiting integrin β5-mediated glycolysis. *Am J Cancer Res*. 2016;6(5):1108-1117.
23. Chen AP, Chu W, Gu YP, Cunnhingham CH. Probing early tumor response to radiation therapy using hyperpolarized [1-^{13}C]pyruvate in MDA-MB-231 xenografts. *PLoS ONE*. 2013;8(2):e56551. https://doi.org/10.1371/journal.pone.0056551
24. Mitov MI, Harris JW, Alstott MC, Zaytseva YY, Evers BM, Butterfield DA. Temperature induces significant changes in both glycolytic reserve and mitochondrial spare respiratory capacity in colorectal cancer cell lines. *Exp Cell Res*. 2017;354(2):112-121. https://doi.org/10.1016/j.yexcr.2017.03.046
25. Sattler UGA, Meyer SS, Quennet V, et al. Glycolytic metabolism and tumour response to fractionated irradiation. *Radiother Oncol*. 2010;94(1):102-109. https://doi.org/10.1016/j.radonc.2009.11.007
26. Hughes P, Marshall D, Reid Y, Parkes H, Gelber C. The costs of using unauthenticated, over-passaged cell lines: how much more data do we need? *Biotechniques*. 2007;43(5):575-586. https://doi.org/10.2144/000112598
27. Döhner H, Estey E, Grimwade D, et al. Diagnosis and management of AML in adults: 2017 ELN recommendations from an international expert panel. *Blood*. 2017;129(4):424-447. https://doi.org/10.1182/blood-2016-08-733196
28. Kreitz J, Schönfeld C, Seibert M, et al. Metabolic plasticity of acute myeloid leukemia. *Cell*. 2019;8(8):805. https://doi.org/10.3390/cells8080805

How to cite this article: Tan JL, Djayakarsana D, Wang H, Chan RW, Bailey C, Lau AZ. Deuterium MRS of early treatment-induced changes in tumour lactate in vitro. *NMR in Biomedicine*. 2021;e4599. doi:10.1002/nbm.4599